PROCEEDINGS OF SPIE

SPIEDigitalLibrary.org/conference-proceedings-of-spie

Automated inline visual inspection and 3D measuring in electrode manufacturing

Andreas Frommknecht, Martin Schmauder, Laura Boonen, Carsten Glanz

Andreas Frommknecht, Martin Schmauder, Laura Boonen, Carsten Glanz, "Automated inline visual inspection and 3D measuring in electrode manufacturing," Proc. SPIE 11056, Optical Measurement Systems for Industrial Inspection XI, 110561Y (21 June 2019); doi: 10.1117/12.2524214

SPIE.

Event: SPIE Optical Metrology, 2019, Munich, Germany

Automated inline visual inspection and 3D measuring in electrode manufacturing

Andreas Frommknecht*[a], Martin Schmauder[a], Laura Boonen[a], Carsten Glanz[a]
[a]Fraunhofer Institute for Manufacturing Engineering and Automation IPA,
Nobelstr. 12, 70569 Stuttgart, Germany

ABSTRACT

Electrode manufacturing is one of the most critical processes within the energy storage production chain, as the electrodes coating and drying quality determines the later performance of the energy storage system in large part. Critical quality losses within the electrode coating are often optical visible, but cannot be automatically and inline inspected. Often small defects like agglomerates, capillary cracks or pinholes in the carbon or metal oxide based layers have to be detected at high web speeds. In the work described in this paper it was examined which kind of features and defects can be recognized by two optical methods: visual inspection and 3D measuring.

A visual camera in conjunction with a white illumination and a 3D data laser line system has been used. Image processing algorithms are applied on the scanned data to detect pinholes and agglomerates. Also thickness of coating, gradient of the coating edge and form anomalies can be determined out of the produced data. Reliable evaluation of pinholes even of small sizes has been proofed. Particle agglomerations are more challenging. To achieve good enough data for 3D evaluation standard sensors are often insufficient, due to the necessary resolution and the production speed that requires high scanning frequency.

In order to provide an automated, digitalized production and inspection system, the devices were coupled to a central experiment management system. Their operation is controlled non-locally in the cloud and synchronized with the execution of experiments. The acquired raw data is stored for later evaluation and long-term archiving.

Keywords: electrode manufacturing, visual inspection, 3D, metrology, inline, digitalization

1. INTRODUCTION

Electrode manufacturing is one of the most critical processes within the energy storage production chain, as the electrodes coating and drying quality determines the later performance of the energy storage system in large part [1]. Defects that arise during the coating process, like agglomerations, pinholes, metal particle contamination, and non-uniform coating will have a significant effect on the later performance of the energy storage device [2]. Especially edge effects can cause problems at the later cell-assembling steps [3]. The edge quality consists of a constant step gradient and the prevention of heavy edges. Especially the first characteristic cannot be measured with conventional coat weight inspection systems. The resolution of radiometric systems or ultrasonic measurement systems (2-4 µm) is often not sufficient to determine the edge quality sufficiently. The detection is additionally hindered by the in general intense difference between the high absorbing coated layers and the reflecting metal foils. Critical quality losses within the electrode coating are often optical visible, but cannot be automatically and inline inspected at higher speed. The uniformity of the wet film can be analyzed by 2D-Laser sensor systems [4], similar to the one used for the in this paper presented 3D measurement (see section 4). Within often carbon or metal oxide based layers that are dark and absorb light very well, small defects like agglomerates of particles, capillary cracks or pinholes in the layer have to be detected at high web speeds. In the work described in this paper it was examined which kind of features and defects can be recognized by two optical methods: visual inspection and 3D measuring.

During the project an experimental plant for electrode manufacturing has been installed [5]. The conveyor speed in the setup is 800 to 1500 $\frac{\text{mm}}{\text{min}}$. The water-based coating is applied by a slot die on the conveyor. After that the coating is dried in the convection dryer of the experimental plant. The coating itself consists mainly of activated carbon which results in a dark black and highly light absorbing surface. The conveyor is a high reflecting thin aluminum foil.

Optical Measurement Systems for Industrial Inspection XI, edited by Peter Lehmann, Wolfgang Osten,
Armando Albertazzi Gonçalves Jr., Proc. of SPIE Vol. 11056, 110561Y · © 2019
SPIE · CCC code: 0277-786X/19/$21 · doi: 10.1117/12.2524214

2. INSPECTION AND MEASUREMENT SETUP

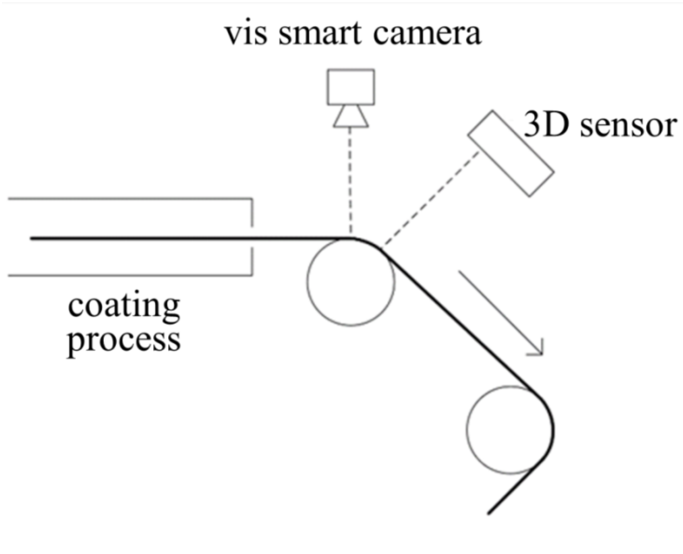

Figure 1 Setup of visual smart camera and 3D sensor in experimental plant

In the experimental plant a visual smart camera and a 3D sensor have been mounted for inspection and measurement tasks, as shown in the sketch in Figure 1. These optical systems are installed after the coating drying section of the plant.

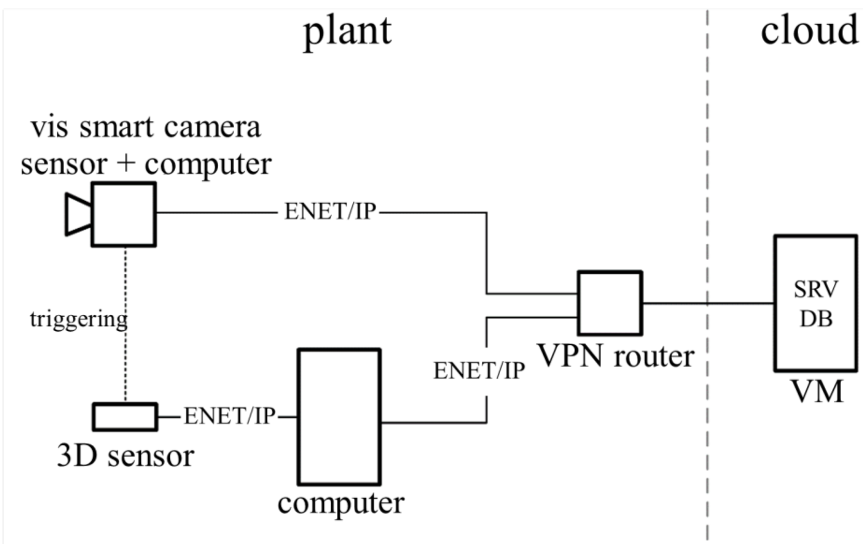

Figure 2 Connections between system components

The different components are connected to each other as shown in Figure 2. A detailed description is given in the following sections.

3. AUTOMATED INLINE INSPECTION AND MEASURING: VISUAL INSPECTION

A visual camera is used in conjunction with a white illumination. Through this in-line system, 500 lines per second are acquired and concatenated to produce a flat image of the coating; image processing algorithms are then applied with the aim of detecting pinholes and agglomerations.

3.1 Requirements

The following list of requirements was deduced:

1. Image acquisition: The acquired visual images, whose quality is mainly controlled by the choice of camera, lens and illumination, shall be appropriate to detect pinholes and particle agglomerates.
2. Device synchronization: In order to enable fusion of the data acquired by the various data sources, precise time information shall be (explicitly or implicitly) attached to the data.
3. Cloud integration: The system shall be remotely controlled and the acquired raw data shall be sent to a cloud-based data store for spatially and timely remote processing.
4. Image processing: Algorithms shall be implemented that are able to detect the quality features in question.

3.2 Implementation

The quality of the acquired images is mainly influenced by the factors camera (spatial resolution and frame rate) and illumination.

Principally speaking, the moving web is acquired a few lines at a time, which are then concatenated to produce a flat image of the coating. A line camera would be ideally suited for the task; for practical reasons, a matrix was used in the project. A smart camera was used for image acquisition. The sensor width is 2592 pixels. The camera was operated at a frame rate of 100 Hz and 4 to 5 lines per image were taken, resulting in an effective line-scan rate of approx. 500 Hz and quadratic pixel projection.

The highly reflecting aluminum foil in combination with the rather matt coating suggests that reliable detection of pinholes can be implemented using a reflected-light illumination strategy. Thus, a white LED ring light was mounted normal to the foil (see Figure 3).

Figure 3 Mounted camera with illumination setup, coated conveyor on roller

In order to guarantee precise synchronization of camera and 3D sensor there are generally two possibilities. In the first case, both of the devices independently attach time-stamps to their acquired data. This, however, leads to the problem of clock synchronization. The respective device clocks do not only have a constant offset, but also a small but non-negligible difference in their factors. Given that due to the acquisition rate, the deviation shall at no time be greater than approx. 1 ms with experiments as long as 2 h, it was not clear how this could be easily guaranteed. It was thus decided to use a direct hardware trigger between the two devices. The camera, itself operating at up to 100 Hz, acts as the master device and generates trigger pulses for the 3D sensor at a frequency of 500 Hz. The electronic components are integrated into the smart camera and no external triggering device was needed. The resulting system has only one clock, avoiding any synchronization problem. The evaluation algorithms can rely on only a time-constant offset between visual and 3D data.

With respect to the cloud integration requirement, a method to transmit and store the acquired images in the cloud was implemented. The basic idea is that a certain number of lines are concatenated and transmitted as a whole. In detail, the camera software, when it acquires an image, first cuts out a certain number of lines (the needed 4 to 5 lines plus a safety margin). It then concatenates a parameterized number of those lines and compresses them using the loss-less PNG data format. Upon completion of a PNG data frame, it is transmitted and saved on permanent storage by uploading it to a server in the cloud using the file transfer protocol (FTP). The described functionality was implemented in a multithreaded software that runs on the four-core smart camera.

The algorithm for processing the images consists of the following steps:

1. Image restauration
    a. Restauration of area images
    b. Shading correction
2. Feature detection

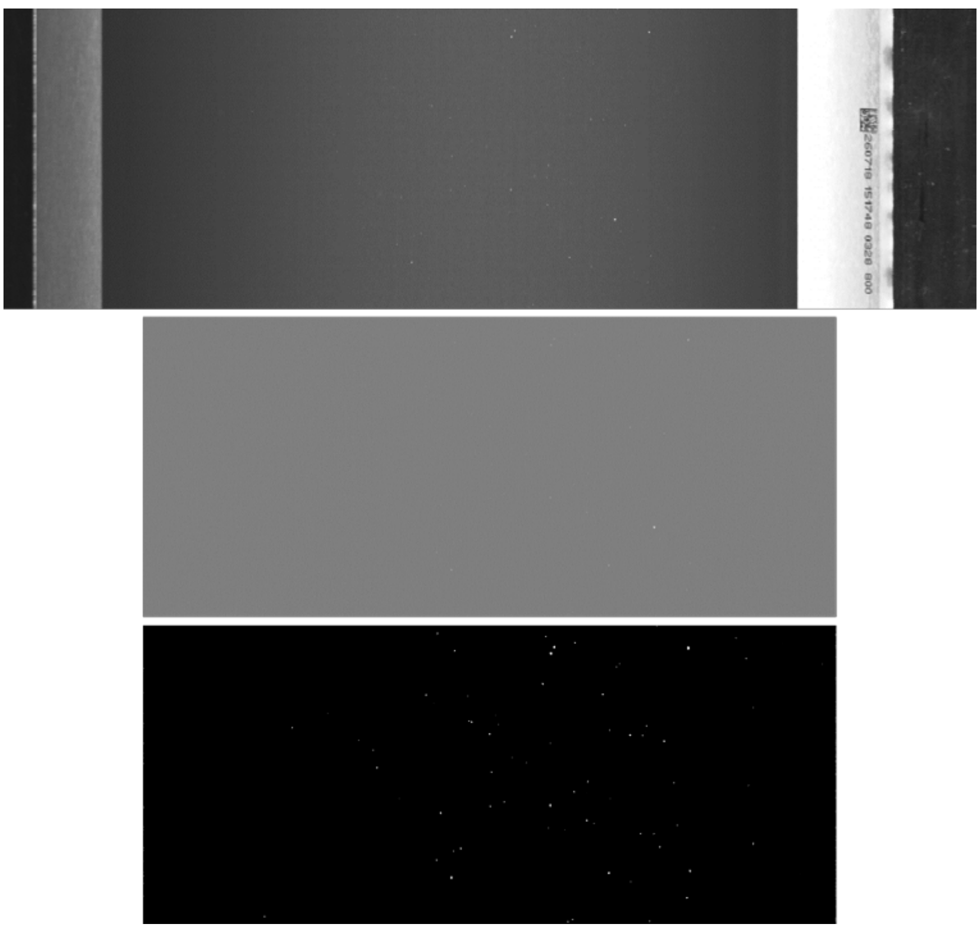

Figure 4 Image processing steps for pinhole counting

In step 1a, four lines of each acquired camera image are cut out and concatenated into area images of a configurable height, a height of 800 was used in the experiments (see Figure 4). As brightness is clearly non-homogeneous across the width of the image, a shading correction filter is applied in step 1b. It is realized using a homogenization filter, which works by dividing each gray value by the median value of its local neighborhood. However, due to the low contrast on the left and right border, effectiveness of image restauration degrades in these areas.

On that basis, the detection of pinholes is simple to implement using a binarization filter, thus separating the bright pinholes from the dark coating. The result of this step is a list of detected pinholes alongside their spatial coordinates on the foil. Area calculation (i. e. counting connected pixels) has also been implemented, but, due to constraints in the optical system, gives reliable results only if defects are big.

In order to detect particle agglomerates, preliminary experiments were conducted that showed that a texture analysis algorithm was capable of reliably detecting the features. However, the coatings that were produced in the final evaluation experiments contained agglomerates of smaller sizes. These smaller features could not be detected, which is presumably not due to the algorithms but to the optical system.

3.3 Results

In a series of experiments, a variety of coatings was produced and inspected. As a result, the pinholes could be reliably detected using the described and implemented image processing algorithms. The applied smart camera provides enough performance to execute even compute-intensive tasks such as PNG compression.

In summary, the adequacy of the basic approach could be demonstrated. Possible improvements mainly include the optical components lens and illumination.

4. AUTOMATED INLINE INSPECTION AND MEASURING: 3D MEASURING

For generating 3D data a laser line system was applied. This sensor is able to scan a height profile. The movement during the electrode manufacturing process allows sticking several profiles together to get the surface of the coating. By evaluating the generated data the thickness of the coating and the gradient of the coating edge can be determined. Furthermore form anomalies can be detected and measured independently of color deviations from its surrounding.

4.1 Used hardware and setup

As 3D sensor a laser line sensor has been chosen. In contrast to stationary systems, as for example fringe projection sensors [6], this type of sensor makes use of the conveyor movement.

Laser line sensors are profile sensors. Each of these profiles consists of several points, where each point consists of a x and z coordinate. While the x coordinate indicates the position of the measured point on the profile line, the z coordinate indicates the height of the point. This set of points is named height profile. The height profiles are calculated directly by the sensor using triangulation between the built-in laser line source and camera. For details of the measuring principle of laser line sensors see [7]. As lasers can be harmful for the human eye, safety measurements have been considered.

The chosen laser line sensor model is a Micro-Epsilon scanCONTROL 2950-25. This sensor was operated in the experimental setup at a frequency of 500 Hz, which means that 500 profiles per second are measured. Application of higher frequencies fails, due to the dark coating (see Figure 5), which implies a high exposure time (increasing exposure time means downsizing of frequency), and the necessary measurement range. In general the resolution of laser line sensors is divided in lateral and vertical resolution, which refers to the above mentioned x and z coordinate. For the applied sensors these values are 20 µm (lateral) und 2 µm (vertical). So the resolution is in the range of state of the art sensors in this field.

To synchronize precisely the 3D sensor to the visual smart camera, a trigger has been installed. The smart camera sends a 500 Hz trigger signal to the laser line sensor (see Figure 2). The sensor itself is connected to a standard computer for evaluation.

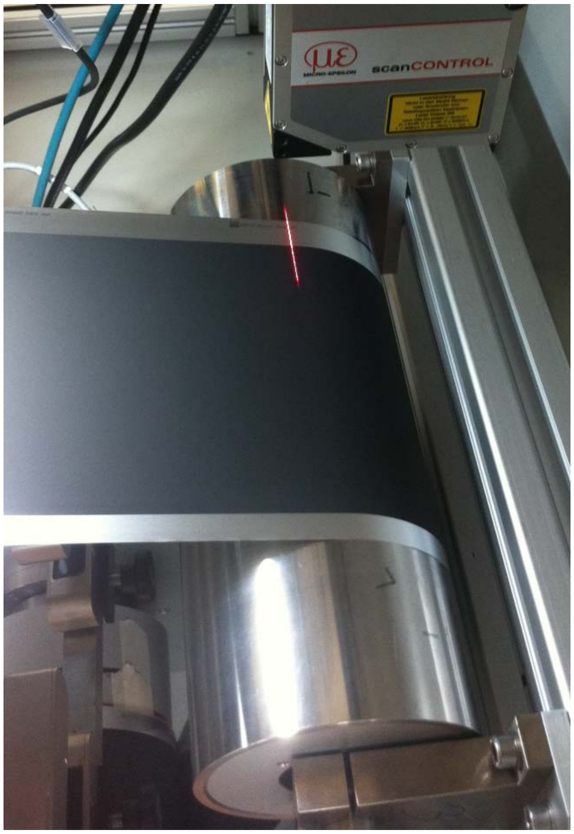

Figure 5 Mounted laser line sensor, coated conveyor on roller

The laser line sensor is mounted as shown in Figure 5. It measures at a position in which the conveyor lies on one of the rollers. This ensures a most stable position without wobbling and a definable zero point (for details see the following sections). Due to the movement of the conveyor different profiles of the coating can be measured by the still standing 3D sensor.

4.2 Evaluation aims

Several defect types and quality features are addressed with the 3D system:

- Missing coating: Occurs e.g. if the nozzle is blocked and can range up to several square millimeters.
- Agglomeration: Accumulations in the coating, which could, depending on the size and amount, influence the quality.
- Coating thickness: The coating thickness is 40 to 150 µm and should be measured in the micrometer range.
- Edge position: The edge should be at the right position and this position should remain constant.
- Edge gradient: The gradient of the edge should be steep. If it's to flat it can be a defect.

4.3 Generating point cloud

The measuring position on the roller makes the measuring repeatable and allows defining a zero point. Defining a zero point means in this case the calculation of a zero profile, which is done by measuring the conveyor without coating. Averaging several of these profiles defines the zero profile. When coating is started, from each new measured profile this zero profile can be subtracted. By doing so a little skewness of the sensor mounting can be balanced and furthermore the z coordinate of the new calculated profile gives directly the height of the coating.

To achieve 3D information out of the scanned 2D profiles, they are merged. This is done by adding a y coordinate to each profile. If the conveyor speed v and the frequency f of the sensor are constant, also the distance d between neighbored profiles stays constant and can be calculated by the following formula:

$$d = \frac{v}{f}$$

So for each added profile to the 3D data set the y coordinate is increased by d.

Evaluation of 3D data instead of direct profile evaluation is necessary due to white noise and the accuracy of the measurement aims. By evaluating the combined profiles the white noise can be reduced.

As mentioned above the triggering-frequency of the profile measurements by the visual smart camera is 500 Hz. This leads for the two tested conveyor speeds 800 $\frac{\text{mm}}{\text{min}}$ and 1500 $\frac{\text{mm}}{\text{min}}$ to the profile distances listed in Table 1.

Table 1. Profile distance depending on conveyor speed.

Conveyor speed [$\frac{\text{mm}}{\text{min}}$]	**Profile Distance [µm]**
800	26,67
1500	50

The sum of the points (each point consisting of x, y and z coordinate) is called point cloud. In the executed experiments each 500 profiles are merged together to one point cloud. An example for such a point cloud is shown in Figure 6. The coating edge is visible in the middle of the point cloud. By fitting a plane [8] the deviation to this plane can be measured and color coded visualized (see Figure 7, the scale values are in mm). When this fitting method is used for measuring deviations the above explained definition, measurement and calculation of a zero point can be avoided, as long as the conveyor and the coating area are both in the measuring field.

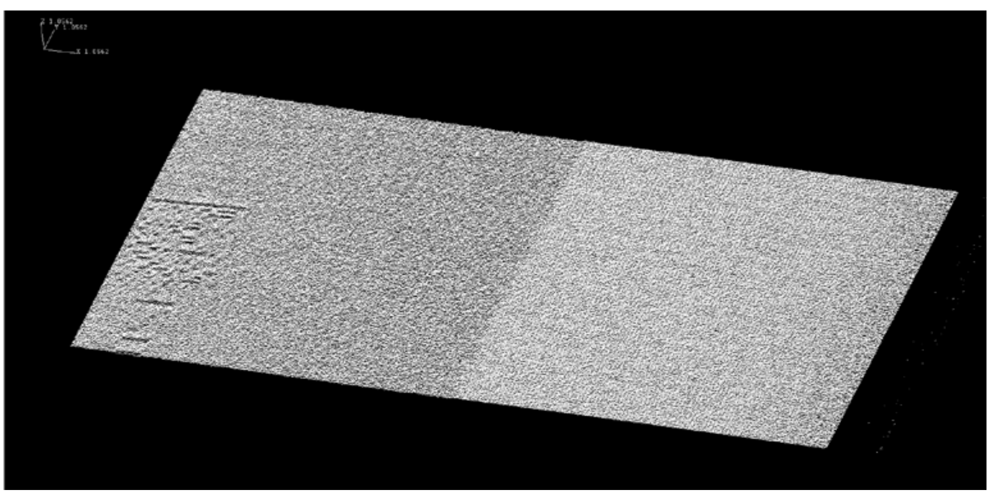

Figure 6 Example of measured point cloud

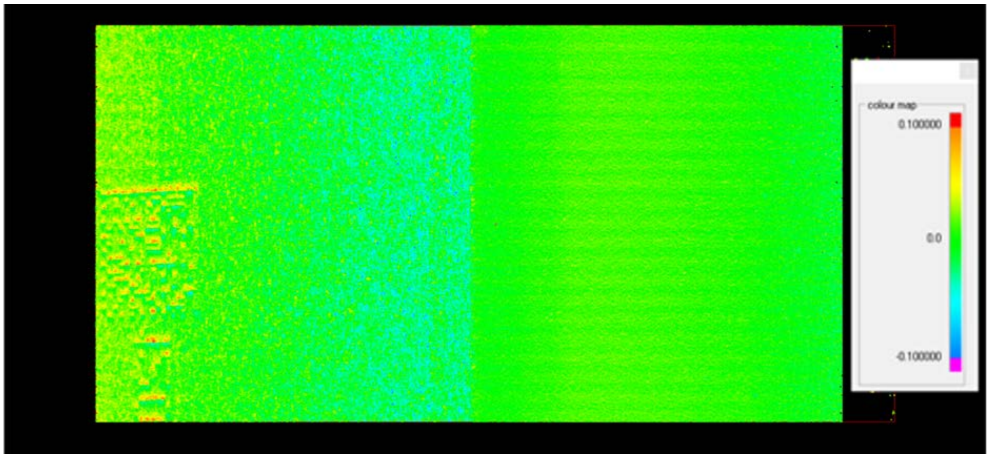

Figure 7 Color coded height deviations

4.4 Conversion into range image and finding coating edge

To achieve the above mentioned aims it's necessary to find the coating edge in the acquired data. Obviously this is necessary for the evaluation of the coating edge, but it's also relevant to separate the coating and the conveyor for the other measurement tasks (missing coating, agglomerations and coating thickness).

The first step of the edge finding is the conversion of each point cloud into a range image, where each gray value corresponds to the measured height (if a zero point has been defined) or the height deviation to the fitted plane (if no zero point has been defined). A detailed description how this conversion, from each 3D point cloud to a gray value image, works can be found in [9]. An example for such an image is shown in Figure 8. Here the edge is already detected and visualized by a white line. For this detection the classical image processing method: Canny Edge Detector [10] with additional implemented filter methods is used with the range image as input data.

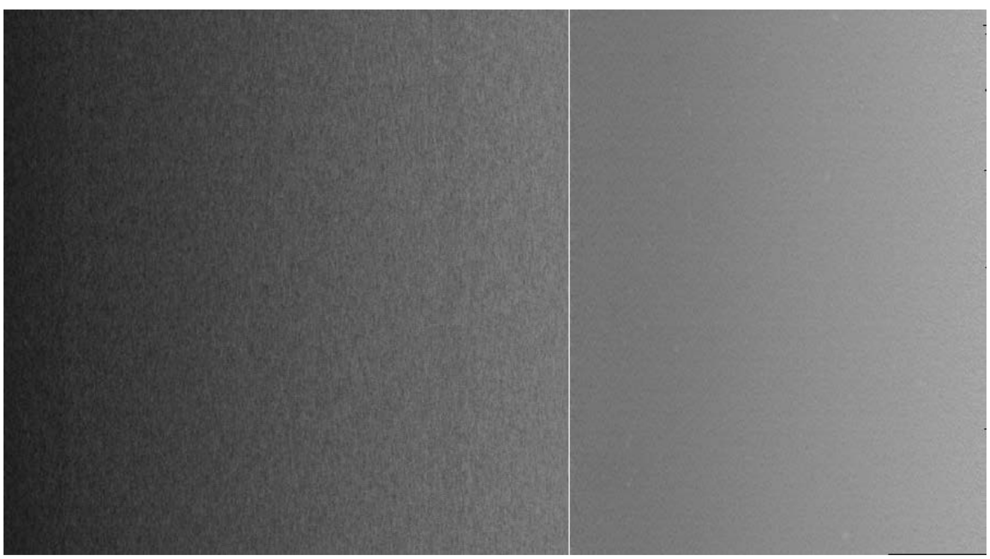

Figure 8 Point cloud converted into range image with detected edge

4.5 Evaluation and results

Each created range image defines one evaluation area (consisting out of 500 profiles) and is used for deriving several measurements results corresponding to the above mentioned evaluations aims: position and gradient of the coating edge, thickness of the coating edge, density of defects with negative and positive height deviations.

The position of the coating edge is a direct result of the finding coating edge procedure. The calculation of the coating edge gradient is a little more complex. For each profile the gradient is calculated. If there's no error the direction of the coating edge is orthogonal to the directions of the profiles. The calculation of the profile gradient works by usage of a user defined distance to the found coating edge and considering the measured height on both sides of the edge. As mentioned above each point cloud consists in the executed experiments out of 500 profiles. To get one gradient for each point cloud the mean of the profile gradients is calculated. This averaging increases the stability of the measurement and calculation and reduces the information to a manageable amount.

For the thickness evaluation the mean of the height of the uncoated conveyor and the mean of the coating height are calculated in the evaluation area. The difference between these two means gives the thickness of the coating.

The density of defects means the amount of negative and positive height deviations divided by the total number of points in the considered area (only the coated part of the evaluation area). A deviation is counted if the difference to the average height in the considered area exceeds a user defined threshold (in the executed experiments 20 µm). If the height of the current point is lower than the average height it's part of defects with negative deviations, if it's higher it's counted as positive height deviation. While high densities of positive height deviations is an indicator for agglomerations, high densities of negative height deviations is an indicator for missing coating or pinholes.

As the sensor is applied with a frequency of 500 profiles per seconds, the evaluation values are updated by each second.

The graph in Figure 9 shows one evaluation example. Here the edge position depending on the time step in seconds removed from outliers over a time period of 1.65 hours is presented. After a run-in time in which the edge position decreases, it remains nearly constant. So by using the evaluation results, the run-in time until a stable condition is reached can be determined and optimized. This is just one example how information can be deduced out of the gained inline measurements.

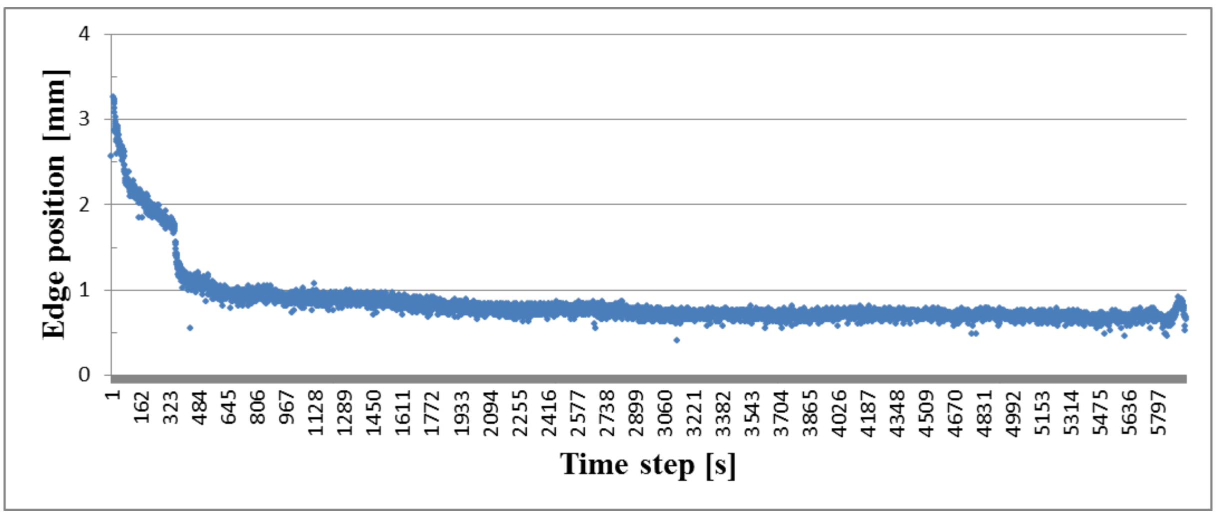

Figure 9 Edge position depending on time step

5. DIGITALIZATION

In order to provide an automated, digitalized production and inspection system, both the visual camera and the 3D height sensor were coupled to a central experiment management system. Device operation is controlled non-locally in the cloud and synchronized with the execution of experiments. The acquired image and 3D information is stored as raw data for later evaluation and long-term archiving.

Going beyond the individual quality assurance systems, the focus was on integration into a digitized complete system. Two aspects were considered:

1. The data provided by the subsystems should be stored in a central location in the cloud and be available for independent evaluation.

2. Operation of the devices should be controlled by a cloud-based experiment management system.

Both the image data of the visual camera and the data of the 3D sensor are transmitted lossless to the cloud and stored there. In addition to these data, the machine data obtained during the experiments was collected and stored using a time series database. For secure transmission between plant and cloud, a virtual private network (VPN) was used. As especially the smart camera did not have enough computing power for the VPN encryption, an encrypting network router that implemented the encryption independently of the connected devices was applied.

To document the experiments, an existing experiment management system (EMS) was used. This not only allows the setting of static experimental parameters, but also the control of the beginning and end of the experiments. This EMS has been extended to also control the data acquisition of the subsystems with its start and stop events. For this purpose, the respective software of the smart camera and the 3D sensor has been extended by a web service interface that reacts to the events accordingly.

Thus, the developed system is cloud-based in terms of both data storage and operational control.

6. DISCUSSION AND CONCLUSION

The main difference of the in this paper presented solution to the state of the art is the combination of 2D and 3D inline optical measurements methods to get the best of both. Another difference is the cloud connection, which extends the experimental setup to a cyber physical system.

6.1 Visual inspection

The applied visual inspection system is capable of detecting and counting pinholes even of small sizes reliably. Agglomerations of practically occurring sizes proved to be more challenging. Improvements regarding the optical system, especially lens and illumination, might improve the detection in the future.

6.2 3D Measuring

A challenge for the 3D inspection is the needed resolution and the production speed. Already very small defects in the submicron range can reduce the electrodes later performance or long-time stability. The measuring target itself is challenging, because it is a highly absorbing material coated onto a reflecting metal foil, which make sensor parameterization difficult. State of the art sensors are often not adapted to the special requirements of electrode manufacturing.

In the presented work only one coating edge has been inspected (see Figure 5), due to the limited measurement range of the used sensor. Most 3D sensors try to offer measurement fields for a wide range of applications. For usage of laser line sensors in the in this paper addressed area a reduced vertical measurement range could be accepted, if on the contrary the lateral range is extended.

Nevertheless useable results have been achieved also by application of a state of the art sensor in combination with intelligent automated evaluation.

6.3 Inspection and measuring systems for future electrode manufacturing

The development of 3D sensors for dark, light absorbing layers produced by fast roll-to-roll printing processes adapted to the needed measurement range might be necessary. Requirements for future measuring and inspection systems are a high data acquisition frequency to meet the increasing machine speeds. As well as an increased accuracy in the edge regions to control edge quality. Another requirement is a high sensitivity for slight color deviations (higher or lower darkness of the coating) to detect concentration variations and agglomerates in the coating. To meet these requirements the combination and integration of several different sensor systems as well as multiple sensor arrays into one inspection system might be necessary.

From the perspective of data management two points are very important. Fast evaluation and feedback of the analyzed data is necessary to identify coating issues in real time and enable the possibility to react in production accordingly. The second important aspect is a very precise synchronization and allocation of acquired data combined with a high performant data management. Only that allows a consistent traceability of coating characteristics throughout the following process steps and within the final product properties.

7. ACKNOWLEDGMENTS

The work described in this paper, was done in the DigiBattPro BW project, which focused on the digitalization of the whole electrode manufacturing process [5]. We like to thank the Ministry of Economic Affairs, Labour and Housing of Baden-Wuerttemberg for funding this project.

REFERENCES

[1] Kenney, B., Darcovich, K., MacNeil, D. D., Isobel J., "Modelling the impact of variations in electrode manufacturing on lithium-ion battery modules," Journal of Power Sources 213, 391-401 (2012). DOI: https://doi.org/10.1016/j.jpowsour.2012.03.065

[2] Mohanty, D., Hockaday, E., Li, J., Hensley, D. K., Daniel, C., Wood, D. L., "Effect of electrode manufacturing defects on electrochemical performance of lithium-ion batteries: Cognizance of the battery failure," Journal of Power Sources 312, 70-79 (2016).
DOI: https://doi.org/10.1016/j.jpowsour.2016.02.007

[3] Schmitt, M., Scharfer, P., Schabel, W., "Slot die coating of lithium-ion battery electrodes: investigations on edge effect issues for stripe and pattern coatings," Journal of Coatings Technology and Research 11(1), 57-63 (2014). DOI: https://doi.org/10.1007/s11998-013-9498-y

[4] Schmitt, M., Baunach, M., Wengeler, L., Peters, K., Junges, P., Scharfer, P., Schabel, W., "Slot-die processing of lithium-ion battery electrodes—Coating window characterization," Chemical Engineering and Processing: Process Intensification 68, 32-37 (2013). DOI: https://doi.org/j.cep.2012.10.011

[5] Schmauder, M., Boonen, L., Frommknecht, A., Glanz, C., Schulz, F., Yesilyurt, O., "Cloud integration of electrode manufacturing via automated tracking and analysis of machine and quality data," Battery Production Conference, Braunschweig (Germany), Nov. 14 to 16 2018. http://publica.fraunhofer.de/documents/N-525659.html

[6] Zhang, S., "Recent progresses on real-time 3D shape measurement using digital fringe projection techniques," Optics and Lasers in Engineering 48, 149-158 (2010).

[7] Gestel, Van N., Cuypers, S., Bleys, P., Kruth, J.-P., "A performance evaluation test for laser line scanners on CMMs," Optics ans Lasers in Engineering 47, 336-342 (2009).

[8] Ahn, S. J., Effenberger I., Rauh, W., Cho, H. Westkämper, E., "Automatic segmentation and model identification in unordered 3D-point cloud," SPIE Proceedings 4902, Optomechatronic systems III, Stuttgart (Germany), Nov. 12 to 14 2002.

[9] Frommknecht, A., Effenberger, I., "3D Milling edge inspecption of CFRP parts by optical methods," International Symposium on Structural Health Monitoring and Nondestructive Testing, Saarbruecken (Germany), Oct. 4 to 5 2018.

[10] Canny, J., "A Computational Approach to Edge Detection," IEEE Transactions Pattern Analysis Machine Intelligence PAMI-8 (6), 679-698 (1986). DOI: https://doi.org/10.1109/TPAMI.1986.4767851